IL NUOVO CIMENTO **40 C** (2017) 177
DOI 10.1393/ncc/i2017-17177-3

COLLOQUIA: LaThuile 2017

Electroweak and QCD Physics at CMS

D. TROCINO on behalf of the CMS COLLABORATION

Northeastern University, Department of Physics – Boston, MA, USA

received 16 September 2017

Summary. — We present recent standard model measurements performed by the CMS experiment at the LHC, using proton-proton collision data at center-of-mass energies of 7, 8, and 13 TeV. Standard model processes involving jets and electroweak gauge bosons span many orders of magnitude in production cross section. Measurements of high-rate processes provide stringent tests of the standard model and help tune the theoretical predictions and Monte Carlo simulations. Thanks to the unprecedented energy and the integrated luminosity provided by the LHC, rare electroweak processes can also be measured for the first time, such as triboson production and vector boson production through vector boson scattering. In addition, new physics phenomena, even beyond the LHC reach, may manifest as enhancements in the multiboson production rate at high energy. Limits on such possible scenarios are set using an effective field theory with anomalous electroweak gauge couplings.

1. – Introduction

Precision measurements of standard model (SM) processes are an essential part of the Large Hadron Collider (LHC) physics program, because they probe a wide range of quantum chromodynamics (QCD) and electroweak (EW) predictions up to the highest energies available, and they can be used to constrain and improve the theoretical calculations and Monte Carlo (MC) simulations. In addition, a precise knowledge of the cross sections and kinematics of SM processes is crucial to detect any signal of new physics phenomena, which will appear as a deviation from SM expectations.

From 2010 through 2016, the LHC delivered proton-proton (pp) collisions at 7, 8, and 13 TeV for a total integrated luminosity of more than $70\,\text{fb}^{-1}$. In the following, a summary will be presented of the main SM measurements involving jets and vector gauge bosons performed by the CMS experiment.

2. – Jet production

Jet production is a key process to test predictions of perturbative QCD and to estimate nonperturbative (NP) effects, such as hadronization and multiparton interactions (MPI). The CMS Collaboration has performed several differential cross section measurements of inclusive jet and multijet production at all the available energies. Jets are generally reconstructed using the anti-k_{T} algorithm [1], with a size parameter R varying between 0.4 and 0.7, depending on the specific data set and analysis. These measurements, which cover more than 7 orders of magnitude, are compared with theoretical predictions at next-to-leading-order (NLO) QCD and EW accuracy, including corrections for NP effects. An excellent agreement is observed over most of the phase space. *E.g.*, fig. 1 (left) shows the double-differential inclusive jet cross section at $\sqrt{s} = 13\,\mathrm{TeV}$ as a function of the jet transverse momentum (p_{T}) and rapidity (y) [2], compared with prediction from program NLOJET++ [3].

The CMS jet measurements are also used to determine the strong coupling constant α_{S} at very high values of transferred momentum Q [4], as well as to constrain the proton parton distribution functions (PDF) [5]. In particular, events with high-p_{T} and high-$|y|$ jets probe large values of the parton fractional momentum x, where the PDFs are poorly known experimentally. Figure 1 (right) shows the gluon PDF as a function of x at the starting scale $Q^2 = 10^5\,\mathrm{GeV}^2$, comparing results from HERA [6] data and those obtained combining HERA data with CMS inclusive jet measurements at 8 TeV. It can be seen that the CMS data provide an effective constrain at high x.

The very-forward calorimeter CASTOR allows for jet detection in the pseudorapidity region $-6.6 < \eta < -5.2$ [7]. Such high-$|\eta|$ jets probe very low x values, $x \sim 10^{-6}$, where the DGLAP evolution [8] is expected to break down, while other models might provide a better description, *e.g.* the Gribov-Regge theory [9]. Figure 2 shows the jet differential cross section *vs.* p_{T} measured at 13 TeV with CASTOR data, compared

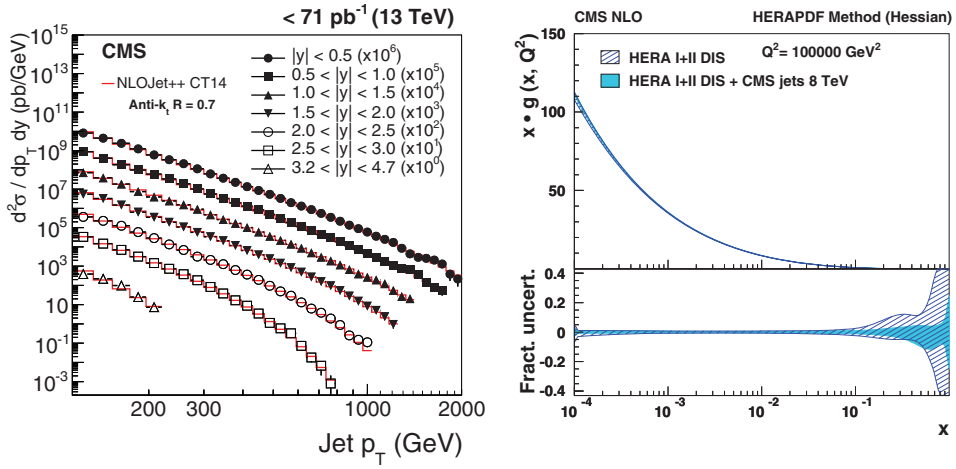

Fig. 1. – Left: double-differential inclusive jet cross section in pp collisions at $\sqrt{s} = 13\,\mathrm{TeV}$, as a function of the jet p_{T} and $|y|$. Right: gluon PDF as a function of x at the starting scale $Q^2 = 10^5\,\mathrm{GeV}^2$, obtained using HERA data only (hatched band) and combining HERA data with CMS inclusive jet measurements at 8 TeV (shaded band).

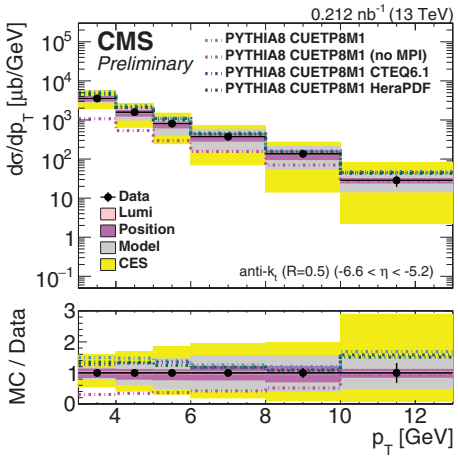

Fig. 2. – Differential jet-p_{T} spectrum in CASTOR, compared to predictions from PYTHIA8 with CUETP8M1 tune and different PDF and MPI models.

with theoretical predictions from PYTHIA8 [10] (based on DGLAP parton evolution) with CUETP8M1 [11] tune and different PDF and MPI models. As can be seen, the experimental uncertainties in the measured cross sections —dominated by the CASTOR energy scale— are currently too large to discriminate among different models. The low-energy region, however, appears to be quite sensitive to the MPI contribution.

3. – W and Z boson production

The inclusive production rate of EW gauge bosons at the LHC is relatively high, and W and Z bosons are used as "standard candles" for multiple purposes, such as detector calibration and lepton efficiency measurement. The production cross sections and kinematic spectra measured at CMS at $\sqrt{s} = 7$, 8, and 13 TeV [12] are in good agreement with NLO and next-to-NLO (NNLO) theoretical calculations, as shown in fig. 3.

The associated production of vector gauge bosons with jets is sensitive to higher-order QCD corrections, but also to soft QCD effects, such as the parton showering. The cross sections and jet kinematics are well reproduced by MC simulations and theoretical calculations at NLO and NNLO (see fig. 4, left) [13]. Measurements of vector boson production in association with heavy-quark jets are also available (*e.g.*, see fig. 4, right) [14].

The EW-induced production of W bosons through vector boson fusion (fig. 5, left) has also been observed [15]. This process is characterized by the presence of two jets at high $|\eta|$, with large rapidity separation and high invariant mass (fig. 5, right). The measured cross section is consistent with leading-order (LO) predictions.

In order to assess the achievable precision on the measurement of the W-boson mass, CMS has performed a preliminary measurement of the Z-boson mass with a "W-like" approach [16], *i.e.* treating either muon from a $\mathrm{Z} \to \mu^+\mu^-$ decay as a neutrino. Thanks to novel calibration algorithms, muon momentum and hadronic recoil are both determined with precisions better than 2×10^{-4}. This is crucial to achieve an experimental uncertainty on the W mass of about 20 MeV, competitive with previous measurements.

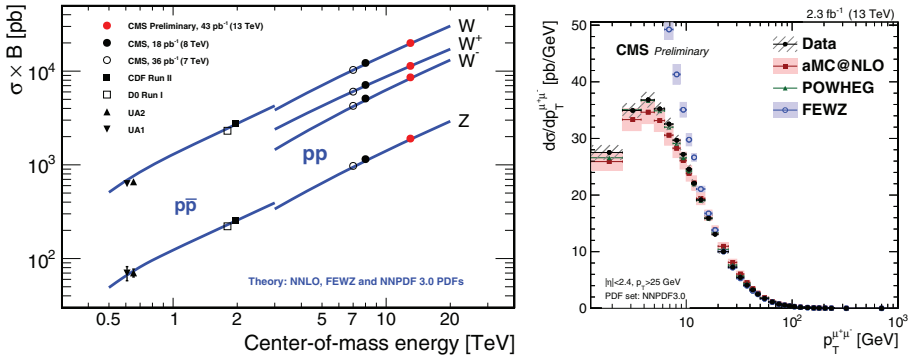

Fig. 3. – Left: measurements of the total W^+, W^-, W, and Z production cross sections times branching fractions *vs.* $\sqrt{s}$ at CMS and other experiments at lower-energy colliders, compared to NNLO theoretical predictions. Right: $Z \to \mu^+\mu^-$ differential cross section as a function of the dimuon p_T, compared to NLO and NNLO calculations.

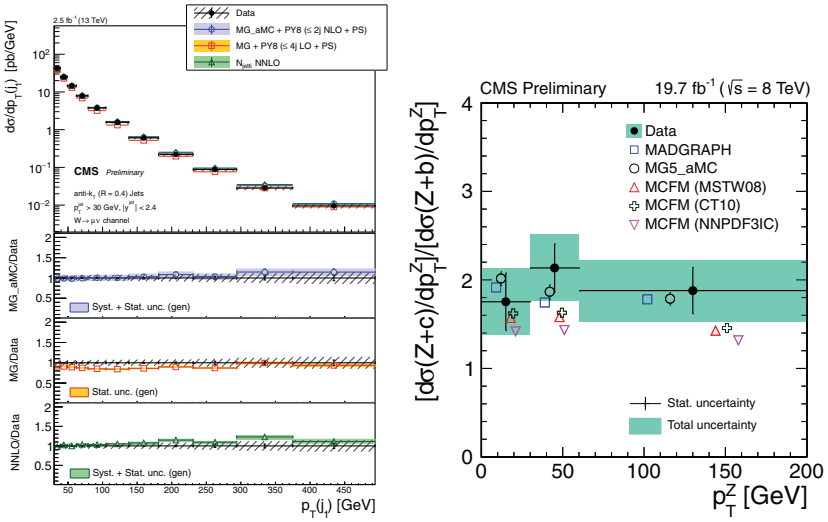

Fig. 4. – Left: differential cross section for the production of a W boson in association with one or more jets, as a function of the leading jet p_T. The measurement is compared to theoretical predictions at NLO and NNLO. Right: ratio of the Z + c quark and Z + b quark differential cross sections, as a function of the Z-boson p_T.

4. – Multiboson production

The measurement of EW-induced multiboson production is a fundamental test of the SM, because it probes the vector boson self-interactions, *i.e.* the existence of triple and quartic gauge couplings (TGC, QGC). Multiboson processes also constitute an irreducible background for many Higgs-boson measurements and new-physics searches, thus a precise knowledge of their cross sections is essential. Any deviation from SM predictions would represent a sign of new physics.

The relatively large diboson production rate at the LHC allows us to select leptonic

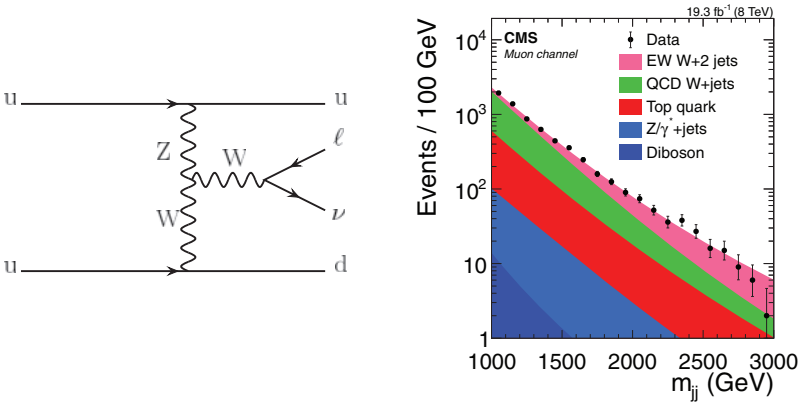

Fig. 5. – Left: a typical Feynman diagram describing the EW-induced production of a W boson via vector boson fusion. Right: distribution of the two-jet invariant mass m_{jj} in $\mu\nu_{\mu}\mathrm{jj}$ events.

final states, characterized by a clean experimental signature and high trigger efficiencies. When possible, hadronic decays are also considered to increase the statistical significance of the measurements. Processes WW, WZ, and ZZ were studied in final states with two, three, or four charged leptons at all available energies. The WW cross section and kinematics prove sensitive to QCD NNLO contributions, partly because of the requirement of a limited number of jets and b-tagged jets applied in the measurement [17]. Also in WZ and ZZ, newly available NNLO calculations improve the agreement with the measured cross sections (see fig. 6) [18].

The exclusive WW production by photon scattering, $\mathrm{pp} \to \mathrm{p}^{(*)}\mathrm{p}^{(*)}\gamma\gamma \to \mathrm{p}^{(*)}\mathrm{p}^{(*)}\mathrm{WW}$, is characterized by the absence of hadronic activity at the primary vertex. This process was measured at 7 and 8 TeV [19] using final states with one electron and one muon, thus suppressing the background from exclusive dilepton production $\gamma\gamma \to \ell\ell$. The observed data are consistent with the SM predictions for this process, and correspond to a signal significance of 3.4 standard deviations (fig. 7, left).

The EW-induced production of $\mathrm{W}\gamma + 2\,\mathrm{jets}$ and $\mathrm{Z}\gamma + 2\,\mathrm{jets}$ through vector boson

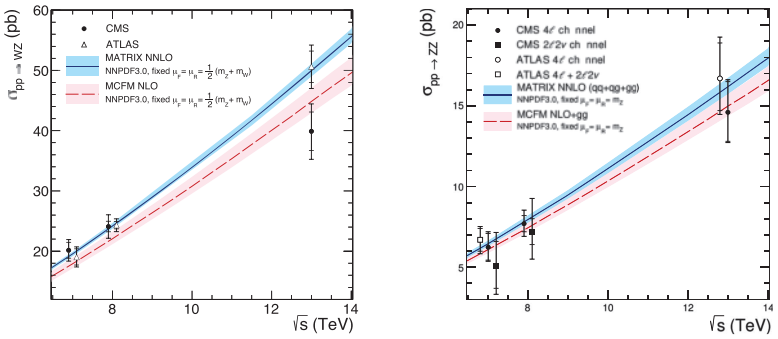

Fig. 6. – The WZ (left) and ZZ (right) total cross sections as a function of the pp center-of-mass energy. Results from the ATLAS and CMS experiments are compared to NLO and NNLO predictions from MCFM and MATRIX, respectively.

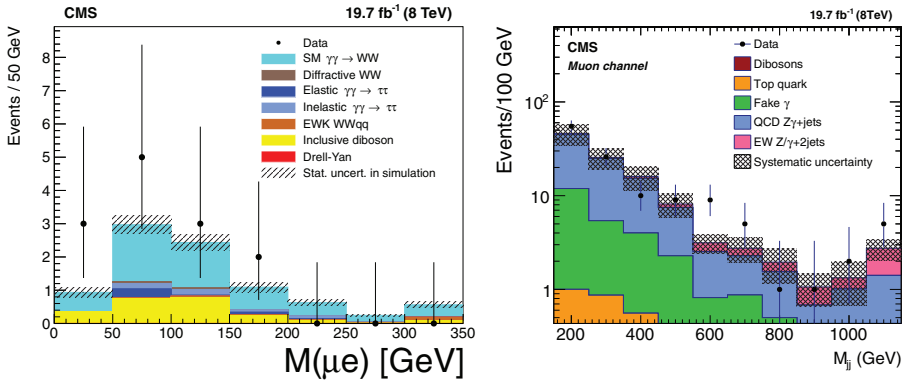

Fig. 7. – Left: muon-electron invariant mass in exclusive $\gamma\gamma \to \mathrm{WW} \to \mathrm{e}\nu_\mathrm{e}\mu\nu_\mu$ production. Right: dijet invariant mass in the EW-induced $\mathrm{Z}\gamma + 2\,\mathrm{jets}$ process.

scattering (fig. 7, right) was also measured at 8 TeV [20], with signal significances of 2.7 and 3.0 standard deviations, respectively. The measured cross sections are in agreement with the SM predictions.

Several triboson processes have been measured in CMS. *E.g.*, fig. 8 shows the p_T of the $\gamma\gamma$ system in $\mathrm{W}\gamma\gamma$ (left) and $\mathrm{Z}\gamma\gamma$ (right) events [21]. As can be seen, the measured data are consistent with the SM expectations, with signal significances of 2.4 and 5.9 standard deviations for $\mathrm{W}\gamma\gamma$ and $\mathrm{Z}\gamma\gamma$, respectively. This represents the first observation of $\mathrm{Z}\gamma\gamma$ production.

5. – Anomalous gauge couplings

The SM predicts precisely the possible self-interactions of gauge bosons. However, new physics phenomena at high energy scales —even beyond the LHC reach— can manifest by modifying the effective vector boson couplings. These effects can be modeled as *anomalous* triple and quartic gauge couplings (ATGC, AQGC) by means of an effective Lagrangian or an effective field theory. Such anomalous couplings generally result in an increase of the multiboson production cross section at high energies, which can be probed

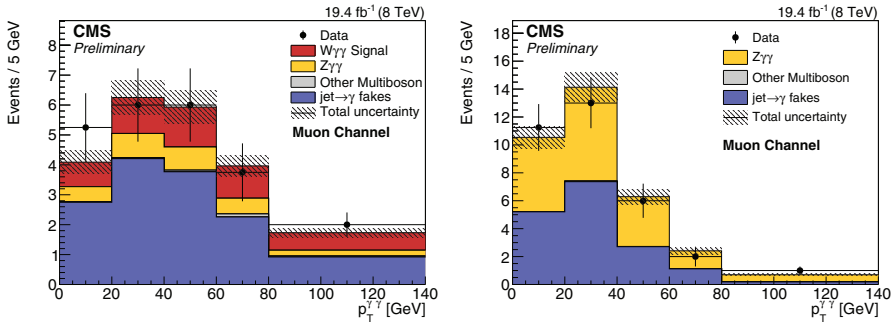

Fig. 8. – Transverse momentum of the diphoton system in $\mathrm{W}\gamma\gamma \to \mu\nu_\mu\gamma\gamma$ and $\mathrm{Z}\gamma\gamma \to \mu\mu\gamma\gamma$ events.

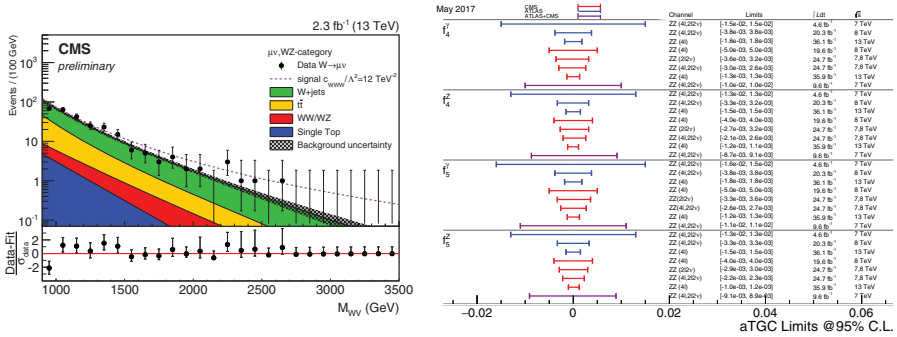

Fig. 9. – Left: WV invariant mass distribution (V = W, Z) in $\mu\nu_\mu$jj events. The dashed line represents the signal yield in the presence of an anomalous WWW coupling. Right: limits on neutral ATGC γZZ and ZZZ obtained by the ATLAS (blue) and CMS (red) experiments with 7, 8, and 13 TeV data.

by analyzing suitable observables, such as the boson p_{T} or the diboson invariant mass. *E.g.*, fig. 9 (left) shows the WV invariant mass (V = W, Z) in events with semileptonic final states, WV $\rightarrow \ell\nu$jj [22]. The dashed line shows the increase in WV rate at high mass in the presence of an anomalous WWW coupling.

In the absence of deviations from the SM expectations, upper limits on the ATGC and AQGC effective parameters can be set. In particular, inclusive diboson measurements help constrain possible ATGC contributions, while triboson and EW-induced diboson processes give access to AQGC. Numerous ATGC and AQGC searches have been performed in CMS using 7, 8, and 13 TeV data. As an example, fig. 9 (right) presents a summary of the ATLAS and CMS limits on neutral ATGC of type γZZ and ZZZ. More results can be found in ref. [23].

6. – Conclusions

A summary was presented of the main QCD and EW measurements conducted at CMS, using LHC data at 7, 8, and 13 TeV. Several (multi)jet differential cross sections have been measured, and constraints on PDFs and α_{S} have been derived. The cross sections and kinematics of W and Z boson production have been studied with very high precision, verifying theoretical calculations up to the NNLO in QCD. Diboson processes have also been measured with increasing precision over the last few years, driving the need for NNLO predictions. Rarer processes, such as triboson, exclusive diboson, or EW-induced (di)boson production are also becoming accessible and the first observations have been achieved. In addition, multiboson measurements have been used to constrain triple and quartic gauge couplings, indirectly probing new physics scenarios with anomalous couplings. The new data that will be delivered by the LHC in the next years will help improve these results, especially by pushing the measurements to ever higher energies.

* * *

The author would like to thank the CMS Standard Model conveners, Mayda Velasco and Kostantinos Theofilatos, and the CMS Forward Physics conveners, Hans Van Haevermaet and Arthur Moraes, for their invaluable help in reviewing these proceedings and the related talk.

REFERENCES

[1] Cacciari M., Salam G. P. and Soyez G., *JHEP*, **04** (2008) 063.
[2] CMS Collaboration, *Eur. Phys. J. C*, **76** (2016) 451.
[3] Nagy Z., *Phys. Rev. Lett.*, **88** (2002) 122003; Nagy Z., *Phys. Rev. D*, **68** (2003) 094002.
[4] CMS Collaboration, CMS-PAS-SMP-16-008.
[5] CMS Collaboration, *JHEP*, **03** (2017) 156.
[6] ZEUS and H1 Collaborations, *Eur. Phys. J. C*, **75** (2015) 580.
[7] CMS Collaboration, CMS-PAS-FSQ-16-003.
[8] Gribov V. N. and Lipatov L. N., *Sov. J. Nucl. Phys.*, **15** (1972) 438; Lipatov L. N., *Sov. J. Nucl. Phys.*, **20** (1975) 94; Altarelli G. and Parisi G., *Nucl. Phys. B*, **126** (1977) 298; Dokshitzer Y. L., *Sov. Phys. JETP*, **46** (1977) 641.
[9] Gribov V. N., *Sov. Phys. JETP*, **26** (1968) 414.
[10] Sjostrand S. M. T. and Skands P., *Comput. Phys. Commun.*, **178** (2008) 852.
[11] Sjostrand T. *et al.*, *Comput. Phys. Commun.*, **191** (2015) 159.
[12] CMS Collaboration, CMS-PAS-SMP-15-004; CMS Collaboration, CMS-PAS-SMP-15-011.
[13] CMS Collaboration, CMS-PAS-SMP-16-005.
[14] CMS Collaboration, CMS-PAS-SMP-15-009.
[15] CMS Collaboration, *JHEP*, **11** (2016) 147.
[16] CMS Collaboration, CMS-PAS-SMP-14-007.
[17] CMS Collaboration, *Eur. Phys. J. C*, **76** (2016) 401.
[18] CMS Collaboration, *Eur. Phys. J. C*, **77** (2017) 236; CMS Collaboration, *Phys. Lett. B*, **763** (2016) 280.
[19] CMS Collaboration, *JHEP*, **08** (2016) 119.
[20] CMS Collaboration, CMS-SMP-14-011; CMS Collaboration, CMS-SMP-14-018.
[21] CMS Collaboration, CMS-PAS-SMP-15-008.
[22] CMS Collaboration, CMS-PAS-SMP-16-012.
[23] CMS Collaboration, `https://twiki.cern.ch/twiki/bin/view/CMSPublic/PhysicsResultsSMPaTGC`.